

UNIVERSITY OF SOUTHAMPTON

**Applications of Microfluidics in Nuclear
Magnetic Resonance**

by

William G Hale

A thesis submitted in partial fulfillment for the
degree of Doctor of Philosophy

in the
Faculty of Engineering and Physical Sciences
School of Chemistry

14/06/2019

UNIVERSITY OF SOUTHAMPTON

ABSTRACT

FACULTY OF ENGINEERING AND PHYSICAL SCIENCES
SCHOOL OF CHEMISTRY

Doctor of Philosophy

by William G Hale

Microfluidics is a constantly growing field of research, finding applications in a diverse range of subjects such as materials science, chemistry and across the life sciences. This expansion is due to many advantageous attributes: small sample volumes which contribute to waste reduction and reduced cost of experimentation; highly controllable local environments that enable very precise investigation of changes in systems to stimuli; rapid prototyping techniques that mean make, test, tweak cycles can be run more than once in a typical day; ease of parallelisation makes gathering statistically significant data much easier without the need to repeat experiments for days at a time; and ease of automation increases precision and repeatability.

Nuclear magnetic resonance (NMR) spectroscopy is a widely applied technique in chemistry and the life sciences. Its non-invasive and non-destructive nature makes NMR ideal to study living, or mass limited samples. NMR, however, requires an extremely homogenous magnetic field to enable molecular structure determination and can be limited by the inherent low sensitivities possible in a typical experiment.

This thesis describes methods for integrating these two fields. Some NMR experiments being ‘miniaturised’ to be performed ‘on-chip’ as well as microfluidic concepts that have been engineered to be compatible with NMR techniques. These techniques do not seek to replace established methods of microfluidic analysis such as mass spectrometry or fluorescence spectroscopy but could be used to compliment these techniques as an additional method of extracting data from a system.

Contents

Nomenclature	iii
Acknowledgements	vi
1 An NMR compatible on-chip Peristaltic Pump	1
1.1 Introduction	1
1.1.1 Materials and Methods	5
1.2 Results and Discussion	6
1.2.0.1 Peristaltics	6
1.2.0.2 Characterisation of flow	8
1.2.1 <i>In situ</i> operation of the device	10
1.3 Conclusions	12
A Appendix	14
A.1 2D Pulse sequences for PH-TOCSY and PH-HMQC	14
A.2 Arduino Firmware	14

Nomenclature

a	The signal amplitude
\mathbb{B}	The Boltzmann factor
B_0	The external magnetic field
B_1	The magnetic field produced by an NMR coil
c_s	The concentration of spins in a sample
C	A constant in SNR
d	The coil diameter
F	The noise factor from the spectrometer
H	The magnetic field
h	Planck's constant
\hbar	The reduced Planck constant
\hat{H}	The Hamiltonian operator in natural units
I	The spin quantum number
\hat{I}	The spin angular momentum operator
i_c	The current
J	The rotational quantum number
k_0	A constant that accounts for spatial inhomogeneities in the B_1 field
k_B	The Boltzmann constant
l	The length of a coil
M_0	The net magnetisation
M_a	The magnetisation vector component along the a -axis
M	The magnetisation
n_s	The number of spins in a sample
$\check{\mathbf{n}}$	The surface normal
p	The polarisation of a spin system
P_α	The population of the α state
R_{noise}	The dissipative loses
\hat{R}	The rotation operator
$S(t)$	The signal in the time domain
$S(\Omega)$	The signal in the frequency domain
T	The absolute temperature
T_1	The longitudinal relaxation time constant

T_2	The transverse relaxation time constant
U	The scalar magnetic potential
V_s	The sample volume
V'_s	The product of k_0 and V_s that is the volume is within 10% of maximum
$\mathbb{1}$	The identity matrix
α_F	The filling factor
β_p	The tilt of the rotation axis from z for an off-resonance pulse
γ_j	The gyromagnetic ratio for a nucleus, j
δ	The chemical shift
δ_{RF}	The RF current penetration depth
Δf	The spectral bandwidth
ϵ	The enhancement factor
θ	The tilt angle of magnetisation
θ_{RF}	The angle between the r.f. coil and B_0
λ_l	The decay constant of a spin l
μ	The reduced mass
μ_0	The vacuum permeability
$\hat{\mu}$	The magnetic dipole moment operator
ξ	The emf
ρ_r	The resistivity
$\hat{\rho}$	The density operator
σ	The chemical shielding factor
ϕ_p	The phase of an r.f. pulse
ϕ_{ref}	The phase shift in the rotating frame
Φ	The angle that connects the static to rotating frame
χ_V	The Magnetic susceptibility
ω_j^0	The Larmour frequency for a nucleus, j
ω_{nutt}	The nutation frequency
ω_{ref}	The rotating frame frequency
Ω^0	The and rotating frame frequency offset

Declaration of Authorship

This thesis is the result of work done wholly while I was in registered candidature for a Ph.D. degree at the University of Southampton. The material presented here is based on work mostly done by myself. Where the work was carried out jointly with others, a substantial part is my own original work and co-workers and their roles have been clearly indicated. The material contained herein has not been submitted by the author for a degree at any other institution.

Signed: 14/06/2019

Acknowledgements

I would like to express my deep gratitude to Professor Marcel Utz for providing patient guidance and enthusiastic encouragement, as well as engaging discussion concerning all matters of life and work. His depth of knowledge in all manner of subjects was a great help throughout my PhD and provided a seemingly endless source of ideas and problem solving. The principles of scientific investigation I have learnt from him will stay with me throughout my career.

I wish to thank Professor Malcolm Levitt for his support and guidance, the discussions we have had about science helped me to see problems in a different light and increased my effectiveness as a scientist.

I am grateful to my colleagues who have helped me enormously throughout my time in Southampton in no particular order I wish to thank: James Eills, Graeme Finch, Rachel Greenhalgh, Benno Meir, Javier Alonso-Valdesueiro, Karel Kouril, Hana Kourilova, Aliko Moysiadi, Stuart Elliot, Christian Bengs, Manvendra Sharma, Bishnubatra Partra, Matheus Rossetto, Gabriel Rossetto, Marek Plata, Sylwia Ostrowska, Weidong Gong, Mohammed Sabba, George Bacanu, Laurynas Dagys, Jo Collel and Barbara Ripka.

To the people that provided support and encouragement throughout my work and helped me keep sane, I am indebted to Frankie Leeming, Thomas Kear, Laura Jowett, James Eills, Stuart Elliot, Christian Bengs, Aliko Moysiadi, Nic Charles, Judy Fox, Josie Charles, Gemma Charles and Eddie Robinson you all helped immensely.

In particular I'd like to thank Alyssa Charles for her unwavering support, encouragement, and belief in me, as well as proof reading and correcting my grammar errors.

Finally, I'd like to thank my family for all their support over the years, this is only possible because of them.

To my friends and family

Chapter 1

An NMR compatible on-chip Peristaltic Pump

1.1 Introduction

The flow and control of liquids in microfluidics is essential, with microfluidic pumping and mixing playing an integral role in many biological and chemical applications, such as DNA analysis [1, 2], protein folding [3], enzyme assays [4, 5], chemical synthesis [6, 7], and kinetic studies [8, 9]. Many solutions to the challenge of pumping and mixing at small scales exist, these include 3D printed valves [10, 11], syringe pumps [12–14], pressure actuated valves [15–17], electrowetting (sometime referred to as digital microfluidics) [18, 19], piezoelectric pumps [20, 21], magnetic pumping [22, 23], and centrifugal forces [24–26].

In this chapter, the design and implementation of an NMR compatible, low dead volume, microfluidic pump will be discussed. The aim of device is to be able to mix two fluids in a controlled manner inside an NMR magnet. It will involve having an on-chip reservoir that can be drawn from and mixed with whichever liquid that is under investigation. These aims are important as the technology could be useful in chemistry applications such as a chemical reaction study, kinetics study, or hyperpolarization on chip. The pump could be used in biological studies too, with protein binding studies already being shown to be possible [27], these pumps could enable whole experiment to be performed on chip. Cell and living tissue culture could also benefit from perfusion provided by the pump, supplying them with fresh O₂ and nutrients. Ultimately, the goal is to observe active changes on the chip, induced by pumping, in real time, using NMR.

Pumps that integrate pumping ‘on chip’ are key to minimising the dead volume within the device. Unger and co-workers [28], were amongst the first to do this by

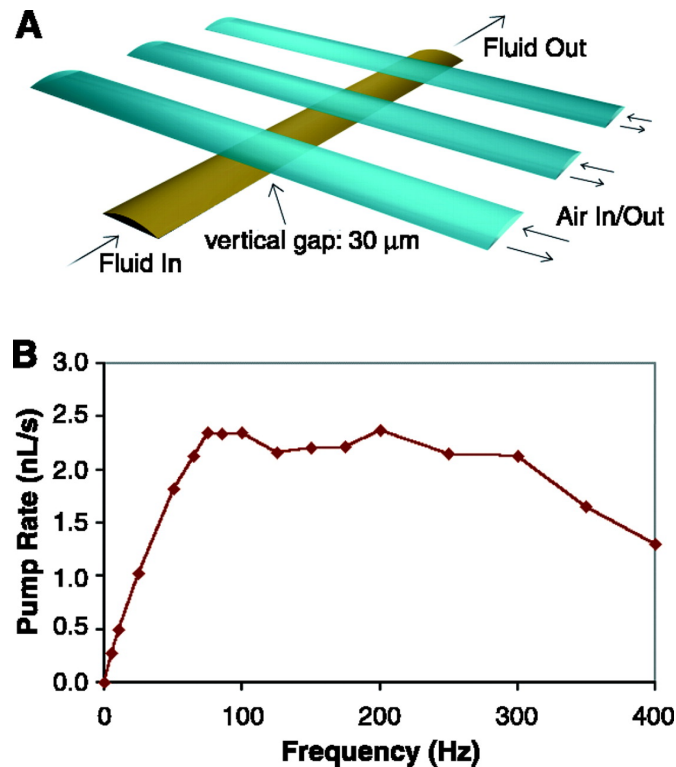


FIGURE 1.1: A) A 3D scale diagram of an elastomeric peristaltic pump. The channels are 100 μm wide and 10 μm high. Peristalsis was typically actuated by the pattern 101, 100, 110, 010, 011, 001, where 0 and 1 indicate “valve open” and “valve closed,” respectively. B) Pumping rate of a peristaltic micropump versus various driving frequencies.

This figure is reproduced from [28].

micro-fabricating PDMS valves using soft lithography. Fig. 1.2 shows the devices, these work by having a central fluid path that has various gas channels running perpendicular above it. By simply applying air pressure, the gas channel expands cutting off the flow in the fluid path beneath. When these valves are actuated in sequence, they produce a net movement of fluid and flow rates of 2.5 nL/s were achieved.

Leslie et al [29] had slightly different approach. In the ‘pump’ the PDMS forms a dome above a circular structure in the fluid channel that is the depressed using air pressure. In order to control the flow they use so called fluidic diodes, these work analogously with electric diodes, by only allowing fluid flow above a certain pressure in one direction only. These diodes are formed by having a weir that separates two fluid channels covered by a compliant PDMS membrane. When the internal fluid pressure reaches the threshold, this pushes the PDMS membrane up and allows fluid connection over the weir. The pressure required to open the diode depends on the thickness of the PDMS ceiling and is predictable which allowed control of flow in the chip at large.

There are specific challenges related to enabling on-chip pumping in a high magnetic field to perform high resolution NMR spectroscopy. Firstly, the materials used should be compatible with a high magnetic field clearly ruling out ferrous metals, this

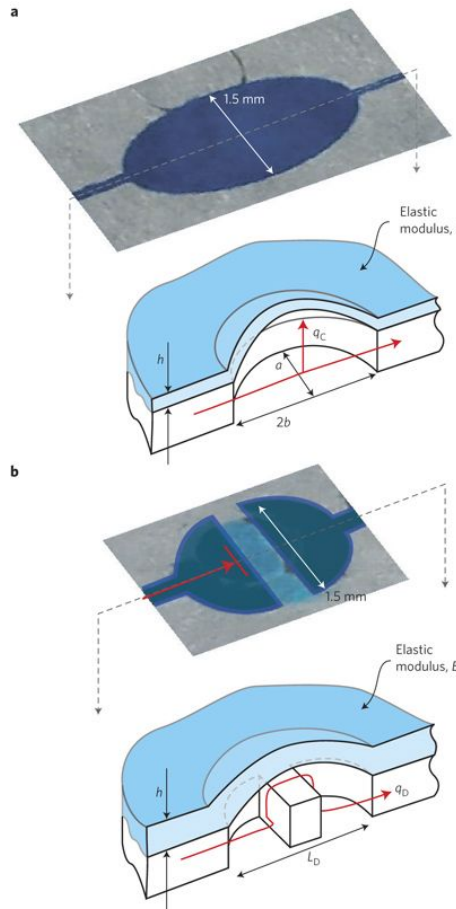


FIGURE 1.2: **a**, Discrete fluidic capacitors are created by bonding deformable films (in this case, PDMS) over reservoirs placed in the network between fluidic channels (resistors) fabricated in glass. These features store and release fluid (volumetric flow rate, q_C) in proportion to the time rate of change in pressure inside the network; the proportionality constant (capacitance, C) depends on film thickness (h), span (a, b) and elastic modulus (E). **b**, Discrete fluidic diodes are created by bonding deformable films around weirs that separate two channels in the network. When the internal pressure is larger than the external pressure, the diode opens and exhibits nonlinear pressure–flow relationships (volumetric flow rate, q_D) dictated by solid–fluid coupling. When the internal pressure is less than the external pressure, the diode pulls shut and prevents flow. Figure taken from [29].

also rules out materials that have a significantly different magnetic susceptibility to that of the chosen fluid (in this case water). As described in chapter ??, susceptibility mismatches need to be carefully managed, or they will interfere with the homogeneity of the magnetic field which is essential for production high resolution spectra. Secondly, materials chosen must also be conducive to rapid prototyping, and as such must be cheap and readily available as well as be easily cut by a laser cutter and bonded using a simple method. These reasons rule out glass, a common microfluidic material, which is not easily cut using a standard laser cutter. Thirdly the chip, when fully assembled, should not be more than 1 mm in thickness, due to limitations imposed by the strip-line probe geometry [30]. This limitation means that more brittle materials, such as glass, would

be too fragile for continuous insertion into the probe and magnet. Lastly, the device should be able to seal against gas and liquid pressures whilst in operation inside the magnet.

With all these limitations, poly(dimethylsiloxane) (PDMS) would seem an ideal candidate. It is: cheap and readily available; easy to cut and bond; and can be made into 1 mm layers to fit the transmission line probe. However, due to its amorphous structure the ^1H background signal is large and broad across the range of ppm that the signals that we are interested in appear. This broad background signal makes it impractical to suppress and any suppression would also suppress the signals that we are interested in, and could lead to difficulties in quantification of substances present in the sample under investigation.

In the design shown, a PDMS layer is still used. However, it is removed from the sensitive area around the sample chamber so that it does not interfere with the signal collected from the device. The 3D printed parts role here is three-fold, firstly, it acts as a conduit for delivering liquids and transporting them around the device. Secondly, it allows for the pressurised air to be delivered which drives the pneumatic valves and enables pumping. Lastly, when screwed together, the 3D printed parts form a seal against liquid and gas leaks.

Nuclear magnetic resonance (NMR) is an ideal tool with which to study live systems, which owing to its non invasive non destructive nature, can give insight into living systems *in situ* and allows for longitudinal studies of them. However, in order to keep these systems alive, and truly replicate *in vivo* conditions, they need fresh supplies of oxygen and nutrients. One way of achieving this is by perfusion of liquid that has been exposed to fresh supplies of oxygen. Perfusion can be accomplished by pumping liquid through the microfluidic device and then out to a reservoir that is in contact with a supply of oxygen. This method would, however, dilute any metabolites given off by the living system that is under investigation within the device, and since the biggest limitation of NMR is sensitivity, it is pertinent to avoid this. This means that the pump would ideally be integral to the device itself. This could reduce the overall volume of the system to tens of microlitres which is much better than the tens of millilitres that come from having an external pumping network. This means that the pump would ideally be integral to the device itself.

In summary, the device must meet the following criteria:

- Non-magnetic parts where possible, susceptibility matched.
- Easily fabricated using rapid prototyping.
- Low dead volume.
- Biocompatible.

- Geometry compatible with transmission line probe.
- Easily assembled and operated *in situ*.

The solution employed here involves a multilayered PMMA device, with two PDMS membranes, sandwiched between two 3D printed holders held together with brass screws. The PMMA device houses the structures for the valves, as well as the fluid circuits, including an NMR sensitive sample chamber and on-chip reservoir. The PDMS layers have two separate functions, the top membrane forms the valves with the PMMA structures whilst the bottom membrane acts as an o-ring to seal against fluid leaks. The 3D printed holders are also multi purpose. The top holder forms the last part of the valves by sealing the PDMS-PMMA valve and allowing the delivery of pneumatic pressure through the bore of the magnet to the device. The bottom 3D printed holder allows the device to be filled and supplies external ports for fluid short circuiting. Together, they help seal the device against gas and liquid leaks. This device coupled with a bespoke, homebuilt probe enables pumping and observation by NMR in a microfluidic device.

1.1.1 Materials and Methods

The devices are composed of three layers of cell cast poly(methyl methacrylate) (PMMA, Weatherall Equipment). The sheet thickness was 200 m for the top and bottom layers, and 500 m for the middle layer. The channels and sample chambers were designed in AutoCAD and cut using a CO₂ laser (HPC Laser Ltd.) to an approximate width and depth of 150 μ m. These layers were bonded together using plasticiser (2.5% v/v dibutyl phthalate in isopropyl alcohol) and subjected to heat and pressure (358 K, 18.6 MPa). To seal the devices, two polydimethyl siloxane (PDMS, Shielding Solutions) were designed in AutoCAD and cut using the same laser as the PMMA layers.

The PMMA and PDMS were screwed together and held in place using 3D printed devices designed in SolidWorks (Acura Xtreme, ProtoLabs). These, as shown in Fig. 1.6, seal the device whilst enabling the filling of the device as well as delivering the pressurised air for the peristaltic pumping.

Firmware for controlling the peristaltic pump was written in Arduino and is provided in the appendix. This has the ability to put the pump into 3 states “advance”, “mixing” and “quiet”. The “advance” state pumps from the outside loop of the device to the inside loop for a desired number of seconds; “mix” pumps around the inner loop for a desired number of seconds; and “quiet” stops all pumping and leaves all valves open indefinitely.

The hardware for controlling pumping comprised of a solenoid valve system with 8 individual valves (Festo, RS). These were connected to 3mm plastic tubes (Festo, RS)

and all supplied from an in-lab air pressure source. This valve system was connected, via a solderless breadboard, to an arduino (Mega 2560, RS) controller allowing for individual control of each of the valves. The Solenoid valve system was powered using a 24V supply.

The device was put into a transmission line based home-built probe. In this, the device is held between two striplines with the inner sample chamber lining up with the constriction on the strip-lines. NMR measurements were performed on a bruker AVANCE III spectrometer and 11.7 T magnet. Spectra were collected using 64 scans using a 90 degree pulse length of 2.5 us at 50 W of power. Water suppression was achieved by using presaturation with 5×10^{-4} W.

100mM solutions of sodium acetate (Merck) and 3-(Trimethylsilyl)-1-propanesulfonic acid (DSS, Merck) by dissolving 82 mg and 196 mg in 10 ml of deionised water (ReAgent) respectively. The two fluidic loops were then filled with these separately and the in/out ports short circuited.

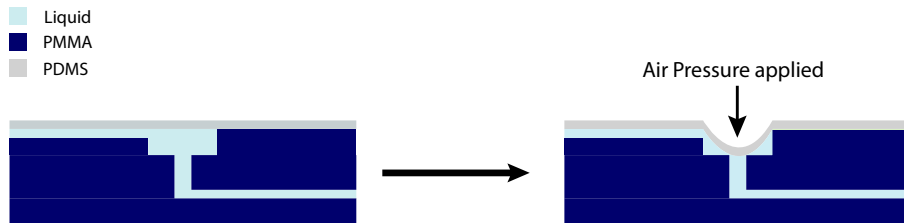


FIGURE 1.3: A cut-through view of the valves in the device showing how when air pressure is applied the PDMS membrane is pushed down and seals the small hole cut in the middle layer.

1.2 Results and Discussion

1.2.0.1 Peristaltics

In order for the dead volume in the device to be kept at a minimum, the valves are implemented in the fluid path on the device itself. Shown below in Fig. 1.3 is the basic principle behind the design.

In the device, there are valves cut into the layers of PMMA. These are formed by two holes in the top and middle layer. The hole in top layer has a radius of $500\mu m$ whilst the hole in the middle layer has a radius of $100\mu m$. The top layer has a channel (approx. $150\mu m$ in width and depth) scored into it to deliver fluid to the top chamber whilst the middle layer has a similar channel scored on the under-side to carry fluid away.

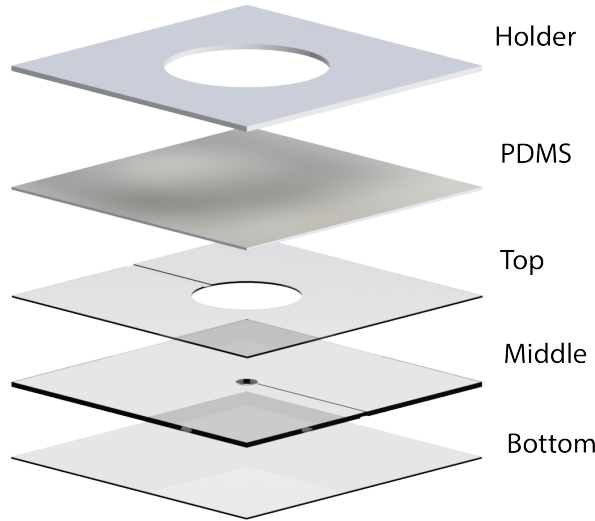


FIGURE 1.4: 3D render of a single valve with 3D printed layer shown too

When covering the hard PMMA structure with the more compliant PDMS membrane of $250\mu m$ thickness, applying air pressure from above seals the valve by covering the hole in the middle layer.

A 3D rendering of a single valve is shown in Fig. 1.4 and shows the ratio of pump holder opening, top hole; and middle hole respectively. The key to these valves is that the scored channels are on opposing sides of the valve.

In Fig. 1.7, micrographs of the chip outside the holders are shown with the valves where one can see the fluid channels on opposing side of their respective layers. Also given, is side by side comparison of the same valve (valve 2 in Fig. 1.5) open (2) and closed (3) one can see the 'ring' formed by the PDMS as it seals against the middle layer.

In my design, there are 6 such valves all individually addressable with air pressure, which when coupled with home-written Arduino firmware, can be actuated in sequence in order to move fluid in a given direction. The block diagram of the arduino set-up is shown in Fig. 1.8. By varying the frequency and lambda parameters, listed in the firmware, one can control the liquid pumped in a given time.

As well as 6 valves, the chips also have two separate liquid circuits that can be connected externally by attaching tubes to the top of the 3D holders as shown in Fig. 1.5. The inner circuit on the diagram contains the pumping network which can be modified to pump around the internal circuit or the complete network, and an NMR sensitive sample chamber where measurements are performed. The external circuit, contains an identical sample chamber that helps to keep the relative volumes of the two circuits

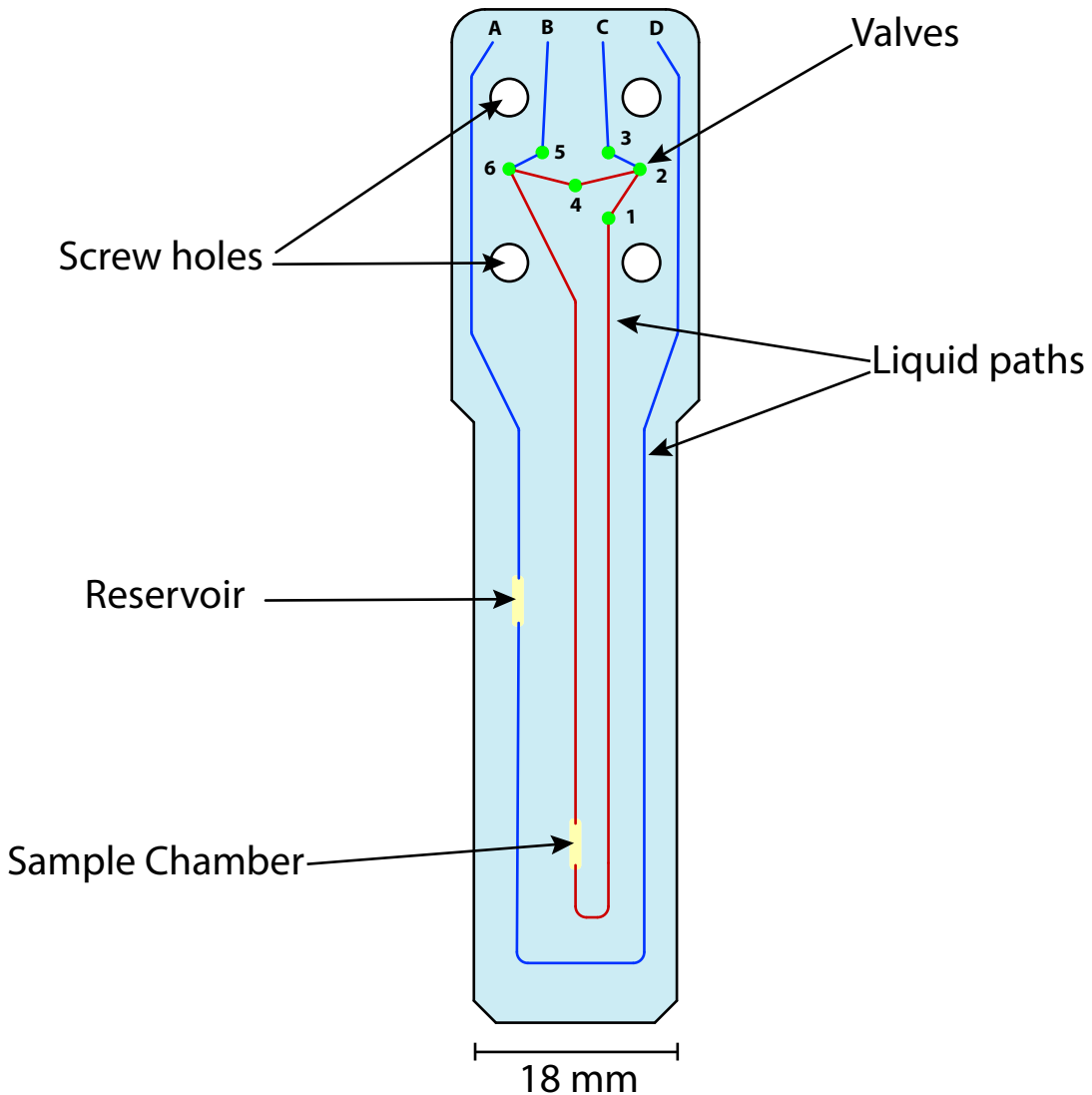


FIGURE 1.5: A CAD drawing of the chip designed for pumping and mixing. Inner (red) and outer (blue) liquid circuits; liquid ports (**A-D**) and valve positions (1-6) shown.

similar. The chip is filled from the ‘bottom’ using the 4 small access holes at the top of the chip (**A-D**). This then allows the valve network and pressurised air to be on the top side of the chip. The challenge in the chip was to fit all the liquid paths and valve network around the 4 large holes in the top of the design which accommodate the screws necessary to hold the device together, and seal against leaks of both liquid and gas.

1.2.0.2 Characterisation of flow

Characterisation of flow experiments were performed with the device in an “open” configuration. This means that after the device was screwed together the two circuits shown in blue and red were joined together by fixing tubing between the **A** and **B** ports

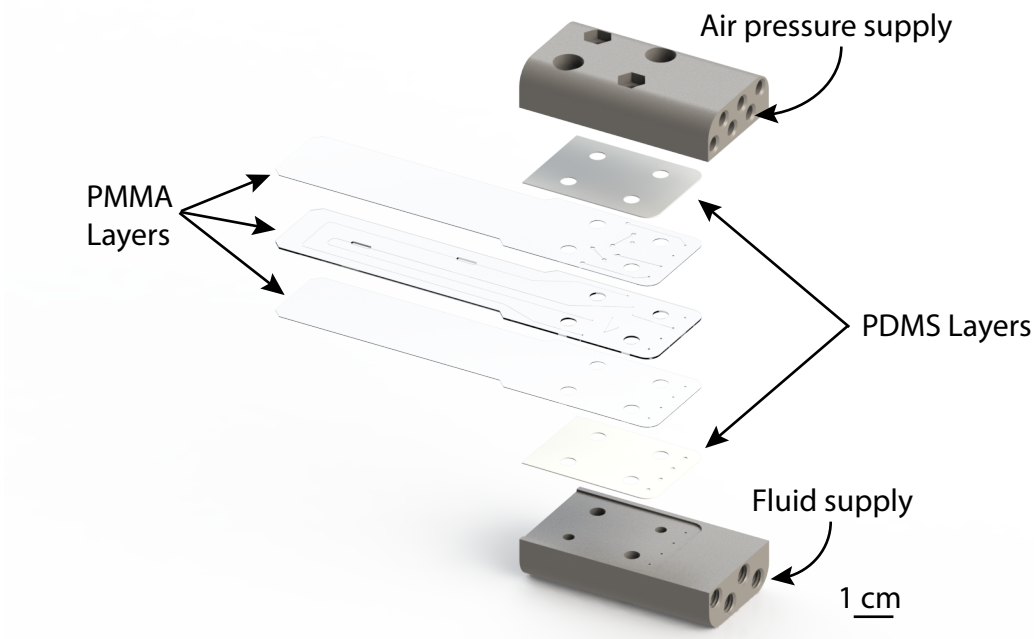


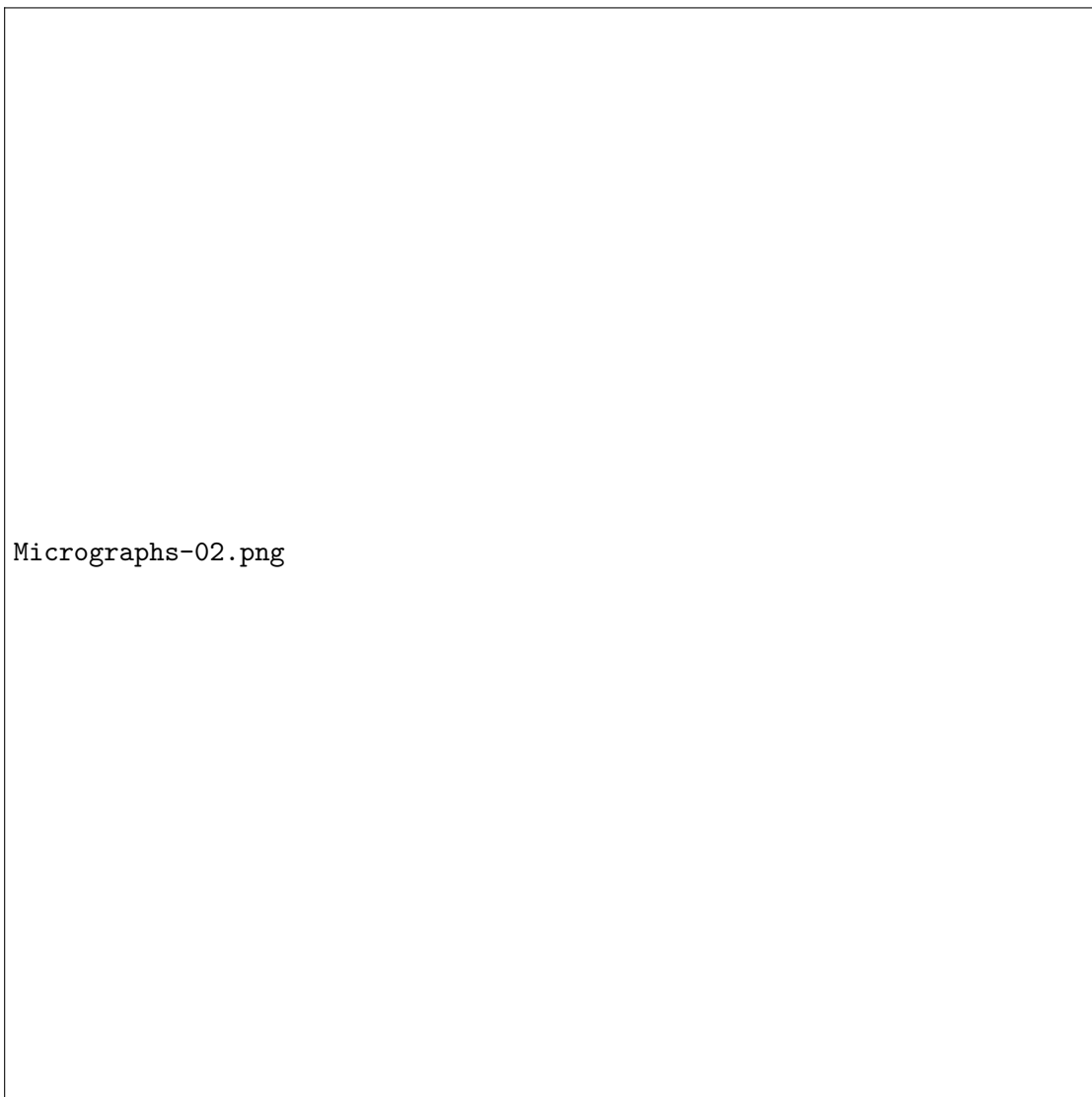
FIGURE 1.6: A 3D representation of the device with separate layers of chips and PDMS layers shown.

shown in Fig. 1.5. This leaves **C** as the “in” port and **D** to be the “out” port with valves 3, 2, and 1 being actuated in sequence to pump, and valve 4 sealed.

The device was connected to translucent polytetrafluoroethylene (PTFE) tubing (Outer diameter 1.6 mm, inner diameter 0.8 mm) with one end submerged in a 500 mL beaker containing filtered DI water (Reagent). Next to the device a ruler was secured to the bench top with the tubing fixed parallel to it. The pump was then switched on and the device allowed to draw water, and pump out the other side. When the water meniscus reached the tubing next to the ruler a timer was started and the distance along the ruler was recorded every minute for 10 minutes. The was repeated 3 times for frequencies from 0.25-1 keeping the lambda constant at 3, which had shown through trial and error to be the optimum number.

The graph shown in Fig. 1.9 is the result of plotting the cumulative volume pumped vs. time. All 4 frequencies show very little deviation from linearity in the long term and also show very small error bars (plotted as $\pm 2\sigma$).

In Fig. 1.10, the flow rate of the pump at varying frequencies is plotted. This shows that the flow rate doesn’t linearly depend on frequency, and seems to level off at higher frequencies. When initially observing the gradient of the lines in Fig. 1.9, the non-linearity was attributed to inconsistencies in the tightening of the screws in the device. However, the small error bars associated with the flow rates across three separate



Micrographs-02.png

FIGURE 1.7: Micrographs of A: free chip showing two valves B: An assembled device with an open valve C: An assembled device with a closed valve, the arrows indicate the area where the PDMS is in contact with the PMMA and is sealing the hole.

experiments, each with at least one disassembly and reassembly of the device, it is now thought that the limit of the pump rate is related to the elasticity of the membrane, and how fast it's able to 'snap back' and re prime itself to pump in each valve.

1.2.1 *In situ* operation of the device

In order to validate the pumps compatibility with NMR, the device was placed into a home built transmission line probe inside a 500 MHz magnet. The arduino controller and solenoid valve bank were secured outside the magnet and the 6 pressurised air lines fed in through the top of the magnet. The device was then filled with 100mM sodium acetate in DI water (Sigma Aldrich) in the inner circuit by attaching a syringe to inlet

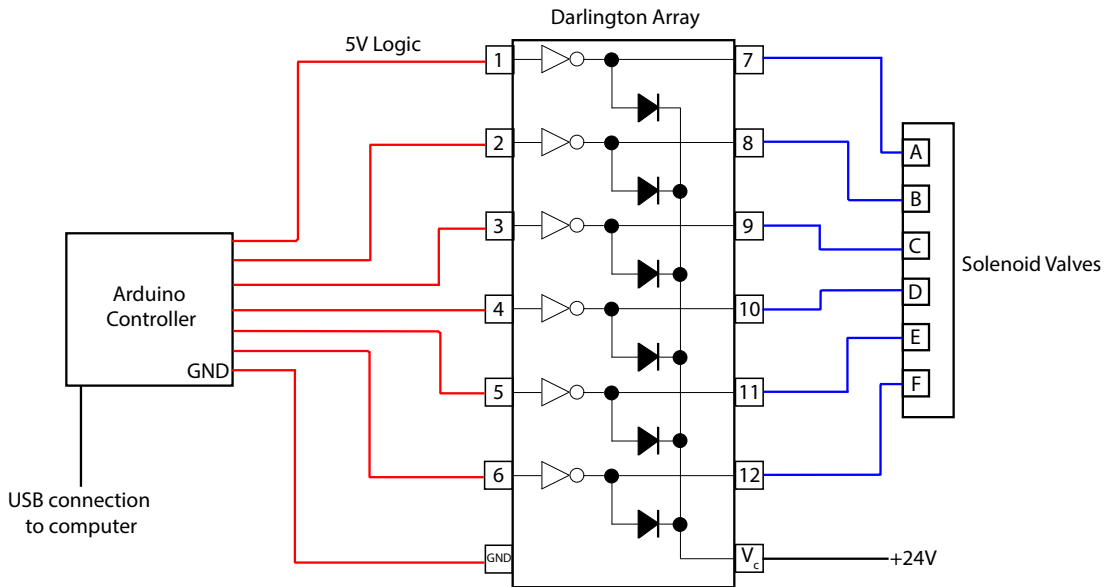


FIGURE 1.8: An arduino controller is connected to, and powered by, a laptop via USB. The controller is connected to a darlington array via six 5V logic connections (shown in red) when addressed, these allow the corresponding pin opposite to draw power from the +24V connected from an outside source. The blue lines indicate the the wires carrying 24V to the solenoid bank which are pneumatically connected to the valves in the chip as labelled.

B in Fig. 1.5. 100mM DSS in DI water (Sigma Aldrich) was added to the outer circuit by syringing into inlet **A**. The sample chamber then contained only sodium acetate and all the initial signal should arise from this. The two fluid networks were then connected using two short lengths of 1/16" outer diameter PTFE tubing by joining **A** to **B** and **C** to **D**.

First, a spectra was collected of the chip after filling, A in Fig. 1.11, using 16 transients and shows mainly the acetate signal at 1.9 ppm. The pump was then put into the 'advance' state for 120 seconds which mean the valves are actuated in order to pump liquid around both circuits. The pump then mixed in the inner circuit for 120 seconds and a second spectra was recorded, B. This shows the 4 signals typical of DSS at 2.91 ppm, 1.75 ppm, 0.63 ppm and 0 ppm and very little acetate signal. Indicating that the volume inside the NMR sensitive area has been almost entirely exchanged. Lastly the pump again advanced and mixed for the same time as before producing the spectra shown in C. Again, this spectrum is different. It shows all signals expected in abundance. This points to mixing of the two substances facilitated by the peristaltic pump and serves as proof, at least in principle, that an NMR compatible microfluidic peristaltic pump capable of mixing liquids in a controllable manor has been presented here.

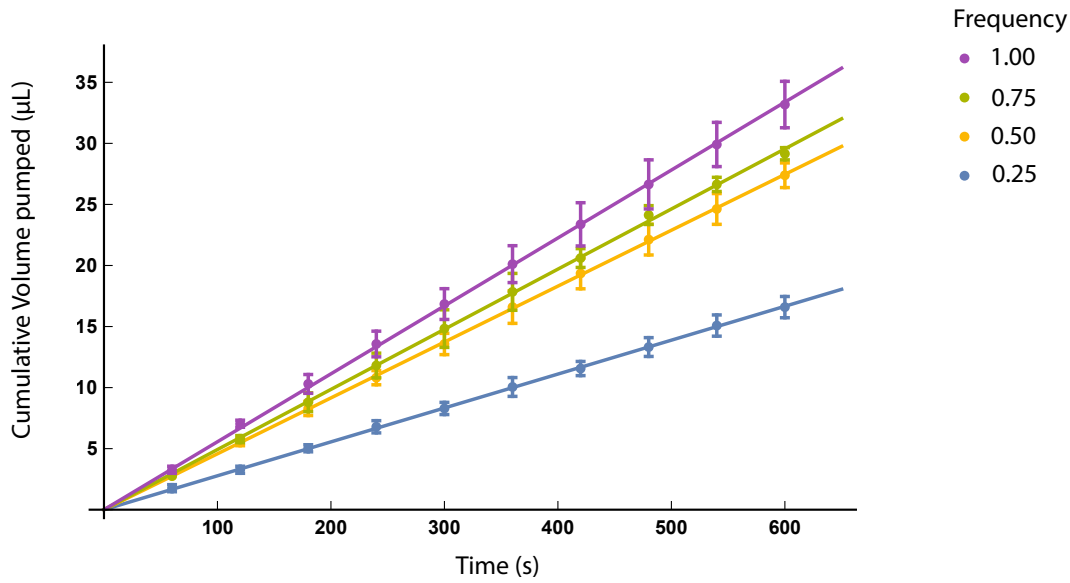


FIGURE 1.9: Plot of the total volume pumped vs time for a chip in the open configuration.

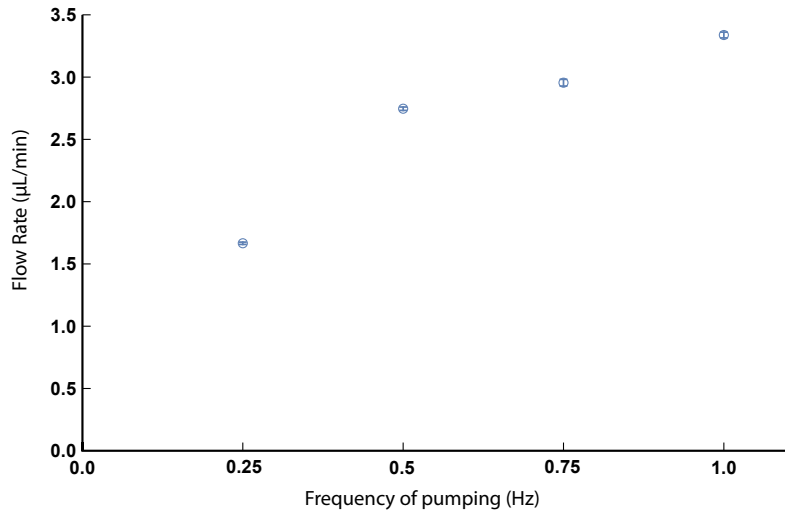


FIGURE 1.10: Flow rates produced by the pump at different frequencies.

1.3 Conclusions

In conclusion, an NMR compatible; low dead volume microfluidic pump has been designed and manufactured that works inside the bore of a high field magnet. The pump has shown excellent linearity and stability in the long term as well as performing exchange, and mixing, of two substances within the device inside a high field magnet. The present limitations are that precise volume control has not yet been achieved. This is,

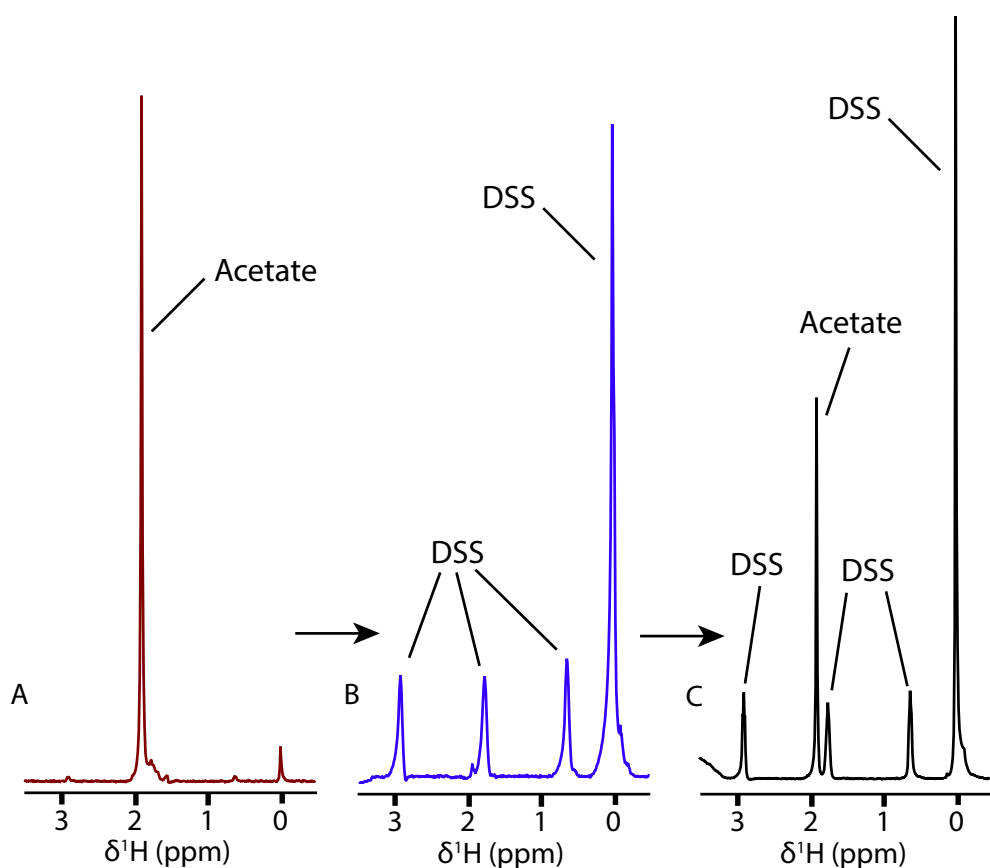


FIGURE 1.11: NMR spectra recorded with 16 transients on a device containing 100mM Sodium acetate in the inner circuit and 100mM DSS in the outer circuit.

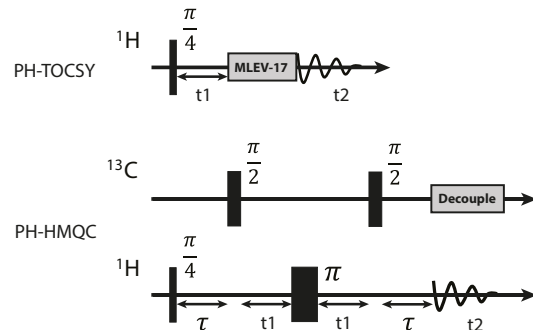
however, thought to be linked with the varied tightening of the screws of the 3D holder as well as the presence of bubbles within the device. Another element that requires further probing is the non-linear dependence of flow rate on frequency. My intuition is that this depends on the thickness of the PDMS layer used however further experimentation with varying thicknesses is needed. Potential future applications of this pump include: microfluidic protein binding experiments; *in situ* liver slice culture and metabolomics; and hyperpolarization experiments.

Appendix A

Appendix

A.1 2D Pulse sequences for PH-TOCSY and PH-HMQC

The pulse sequences used for the PH-TOCSY and the PH-HMQC spectra are shown below.



A.2 Arduino Firmware

Below the firmware for the operation of the peristaltic pump is given.

```
pump_driver_0.0.1

#define VALVE_A 3
#define VALVE_B 11
#define VALVE_C 2
#define VALVE_D 4
#define VALVE_E 5
#define VALVE_F 6
#define N_VALVES 6

int ValvePins[] = {VALVE_A, VALVE_B, VALVE_C, VALVE_D, VALVE_E, VALVE_F};
```

```
int AdvancePump[] = {VALVE_A, VALVE_B, VALVE_C};
int AdvanceValves[] = {LOW, LOW, LOW, HIGH, LOW, LOW};

int MixPump[] = {VALVE_F, VALVE_D, VALVE_B};
int MixValves[] = {HIGH, LOW, LOW, LOW, HIGH, LOW};

long bedTime = 0;

enum state {QUIET, MIX, ADVANCE};

String stateDesc[] = {"idling.", "mixing", "pumping"} ;

state currentState;
state lastState;

const int MaxParams = 5;
String command;
String params[MaxParams];
int nparam=0;

float freq = -1.0;
float lambda = 3.0;

void setup() {

    for(int k=0;k<N_VALVES;k++)
    {
        pinMode(ValvePins[k], OUTPUT);
        digitalWrite(ValvePins[k], LOW);
    }

    Serial.begin(115200);
    while(!Serial);
    Serial.println("Hello.");
}

void loop() {
    if( checkForCmd() ) processCmd() ;
    if( millis() > bedTime ) gotoState(QUIET);

    switch (currentState) {
        case MIX :
            startPump(MixPump,3,freq,lambda) ;
            break ;

        case ADVANCE :
            startPump(AdvancePump,3,freq,lambda) ;
            break;

        default:
            break;
    }

    delay(10);
}
```

```
void gotoState(state newState)
{
    if(currentState != newState) {
        lastState = currentState;
        currentState = newState;

        Serial.print(stateDesc[newState]);

        switch(newState) {
            case MIX:
                for(int k=0;k<N_VALVES;k++) digitalWrite(ValvePins[k],MixValves[k]);
                Serial.print(" for ");
                Serial.print((bedTime-millis())/1000.0);
                Serial.println(" seconds.");
                break;

            case ADVANCE:
                for(int k=0;k<N_VALVES;k++) digitalWrite(ValvePins[k],AdvanceValves[k]);
                Serial.print(" for ");
                Serial.print((bedTime-millis())/1000.0);
                Serial.println(" seconds.");
                break;

            case QUIET:
                for(int k=0;k<N_VALVES;k++) digitalWrite(ValvePins[k],LOW);
                Serial.println();
                break;
        }
    }

    bool checkForCmd()
    {
        if(!Serial.available()) return(false);

        command = Serial.readStringUntil('\n');
        command.trim();
        int k;
        do {
            k=command.indexOf(' ');
            params[nparam++] = command.substring(0,k);
            command=command.substring(k);
            command.trim();
        } while(k>0 && nparam < MaxParams) ;

        /* Serial.println("command read."); */

        return(true);
    }

    void processCmd()
    {

        command="";

        /* for(int k=0;k<nparam;k++) {
            Serial.println(params[k]);
        }*/
    }
}
```

```
    } */

    if(npParam>0) {

        if(params[0]==="mix") {
            bedTime = millis() + params[1].toFloat()*1000;
            gotoState(MIX);
        }

        else if (params[0]==="adv") {
            bedTime = millis() + params[1].toFloat()*1000;
            gotoState(ADVANCE);
        }

        else if(params[0]==="stop") {
            gotoState(QUIET);
            bedTime = millis();
        }

    }

    npParam=0;
}

void startPump(int *valves, int npins, float freq, float lambda)
{
    float psi;
    for(int k=0;k<npins;k++) {
        psi=cos( 2*PI*(k/lambda-freq*millis()/1000.) );
        if(psi>0)
            digitalWrite(valves[k],HIGH) ;
        else
            digitalWrite(valves[k],LOW);
    }
}

void stopPump(int *valves, int npins)
{
    for(int k=0;k<npins;k++)
        digitalWrite(valves[k],LOW);
}
```

Bibliography

- [1] J. Liu, B. A. Williams, R. M. Gwirtz, B. J. Wold and S. Quake, *Angewandte Chemie International Edition*, 2006, **45**, 3618–3623.
- [2] S. Huang, C. Li, B. Lin and J. Qin, *Lab on a Chip*, 2010, **10**, 2925–2931.
- [3] L. Jiang, Y. Zeng, Q. Sun, Y. Sun, Z. Guo, J. Y. Qu and S. Yao, *Analytical Chemistry*, 2015, **87**, 5589–5595.
- [4] I. N. Kefala, V. E. Papadopoulos, G. Karpou, G. Kokkoris, G. Papadakis and A. Tserepi, *Microfluidics and Nanofluidics*, 2015, **19**, 1047–1059.
- [5] A. G. Hadd, D. E. Raymond, J. W. Halliwell, S. C. Jacobson and J. M. Ramsey, *Analytical Chemistry*, 1997, **69**, 3407–3412.
- [6] M. C. Mitchell, V. Spikmans and A. J. de Mello, *Analyst*, 2001, **126**, 24–27.
- [7] H. Kim, K.-I. Min, K. Inoue, D.-P. Kim and J.-i. Yoshida, *Science*, 2016, **352**, 691–694.
- [8] H. Fang, Y. Sun, X. Wang, M. Sharma, Z. Chen, X. Cao, M. Utz and Z. Tian, *Science China Chemistry*, 2018, **61**, 1460–1464.
- [9] A.-L. Liu, Z.-Q. Li, Z.-Q. Wu and X.-H. Xia, *Talanta*, 2018, **182**, 544–548.
- [10] H. Gong, A. T. Woolley and G. P. Nordin, *Lab on a Chip*, 2016, **16**, 2450–2458.
- [11] A. K. Au, N. Bhattacharjee, L. F. Horowitz, T. C. Chang and A. Folch, *Lab on a Chip*, 2015, **15**, 1934–1941.
- [12] A. Terray, J. Oakey and D. W. Marr, *Science*, 2002, **296**, 1841–1844.
- [13] Z. Li, S. Y. Mak, A. Sauret and H. C. Shum, *Lab on a Chip*, 2014, **14**, 744–749.
- [14] T. Ward, M. Faivre, M. Abkarian and H. A. Stone, *Electrophoresis*, 2005, **26**, 3716–3724.
- [15] M. A. Unger, H.-P. Chou, T. Thorsen, A. Scherer and S. R. Quake, *Science*, 2000, **288**, 113–116.

- [16] V. Studer, G. Hang, A. Pandolfi, M. Ortiz, W. French Anderson and S. R. Quake, *Journal of applied physics*, 2004, **95**, 393–398.
- [17] C. Vicider, O. Ohman and H. Elderstig, Proceedings of the International Solid-State Sensors and Actuators Conference-TRANSDUCERS'95, pp. 284–286.
- [18] A. R. Wheeler, *Science*, 2008, **322**, 539–540.
- [19] W. Cui, M. Zhang, X. Duan, W. Pang, D. Zhang and H. Zhang, *Micromachines*, 2015, **6**, 778–789.
- [20] Y. Oda, H. Oshima, M. Nakatani and M. Hashimoto, *Electrophoresis*, 2019, **40**, 414–418.
- [21] C. H. Chen, S. H. Cho, F. Tsai, A. Erten and Y.-H. Lo, *Biomedical microdevices*, 2009, **11**, 1223.
- [22] A. Hatch, A. E. Kamholz, G. Holman, P. Yager and K. F. Bohringer, *Journal of Microelectromechanical systems*, 2001, **10**, 215–221.
- [23] J. Belardi, N. Schorr, O. Prucker and J. Rühe, *Advanced Functional Materials*, 2011, **21**, 3314–3320.
- [24] B. S. Lee, Y. U. Lee, H.-S. Kim, T.-H. Kim, J. Park, J.-G. Lee, J. Kim, H. Kim, W. G. Lee and Y.-K. Cho, *Lab on a Chip*, 2011, **11**, 70–78.
- [25] S. T. Krauss, T. P. Remcho, S. M. Lipes, R. Aranda IV, H. P. Maynard III, N. Shukla, J. Li, R. E. Tontarski Jr and J. P. Landers, *Analytical Chemistry*, 2016, **88**, 8689–8697.
- [26] B. S. Lee, J.-N. Lee, J.-M. Park, J.-G. Lee, S. Kim, Y.-K. Cho and C. Ko, *Lab on a Chip*, 2009, **9**, 1548–1555.
- [27] G. Finch, A. Yilmaz and M. Utz, *Journal of Magnetic Resonance*, 2016, **262**, 73–80.
- [28] M. A. Unger, H.-P. Chou, T. Thorsen, A. Scherer and S. R. Quake, *Science*, 2000, **288**, 113–116.
- [29] D. C. Leslie, C. J. Easley, E. Seker, J. M. Karlinsey, M. Utz, M. R. Begley and J. P. Landers, *Nature Physics*, 2009, **5**, 231.
- [30] M. Sharma and M. Utz, *Journal of Magnetic Resonance*, 2019, **303**, 75–81.